IOPscience iopscience.iop.org

Home Search Collections Journals About Contact us My IOPscience

Visible and infrared optical properties of Ag/SiO_2 multilayers: radiative virtual modes and coupling effects

This article has been downloaded from IOPscience. Please scroll down to see the full text article.

1993 J. Phys.: Condens. Matter 5 7361

(http://iopscience.iop.org/0953-8984/5/40/011)

View the table of contents for this issue, or go to the journal homepage for more

Download details:
IP Address: 171.66.16.96
The article was downloaded on 11/05/2010 at 01:56

Please note that terms and conditions apply.

J. Phys.: Condens. Matter 5 (1993) 7361–7374. Printed in the UK

Visible and infrared optical properties of Ag/SiO_2 multilayers: radiative virtual modes and coupling effects

A Bichri, J Lafait and H Welsch

Laboratoire d'Optique des Solides de l'Université Pierre et Marie Curie, UA au CNRS No 781, 4 Place Jussieu, 75252 Paris Cédex 05, France

Received 9 June 1993, in final form 21 July 1993

Abstract. Optical measurements (photometry and ellipsometry) were performed under oblique incidence from 0.03 eV to 6 eV on silver/silica (Ag/SiO_2) multilayers prepared by magnetron sputtering. Around 3.78 eV, the plasma frequency of Ag, and 0.154 eV and 0.133 eV, the longitudinal and transverse optical frequencies of SiO_2, resonances are observed, characteristic of the Ferrell and Berreman modes in single Ag and SiO_2 layers. These modes and a Brewster mode observed around 3.87 eV are weakly influenced by the SiO_2 thickness in the multilayers. Below 3.78 eV, strong coupling effects between surface plasmon modes at the metal/dielectric interfaces generate a transparency window with low reflectance, whose width is well described within the effective medium approximation.

1. Introduction

Metal/dielectric multilayers have undergone intensive development in recent years due to their utilization in the x-ray and neutron ranges as reflectors, monochromators and polarizers [1,2]. However, very few publications concern their optical properties in the visible and infrared ranges. Their potential applications in these domains are nevertheless interesting due to resonances and coupling effects which can strongly modify their optical response and induce a strong anisotropy.

In single metallic or dielectric layers resonances occur at or near characteristic frequencies: the plasma frequency ω_p of the metal, and the longitudinal optical frequency ω_l of the dielectric. At these frequencies, radiative surface plasmon modes (Ferrell modes) and radiative surface phonon modes (Berreman modes) can be excited in the metallic and dielectric layers respectively, under oblique incidence, for p-polarized light (electric field parallel to the plane of incidence).

In a metal/dielectric multilayer coupling effects throughout the multilayer may enhance or weaken these resonances already predicted and observed in metallic or dielectric single layers. Moreover, the coupling between radiative surface plasmon modes can give rise to propagative modes with bulk like character, which is manifested by a transparency window with low reflectance.

In this work we demonstrate experimentally these effects on silver/silica (Ag/SiO_2) multilayers with a limited number of layers and we interpret their optical properties from the near ultraviolet to the far infrared.

We first recall in section 2 the theoretical framework necessary to this interpretation: radiative modes in metallic and dielectric single layers; and the effective medium approximation (EMA) for periodic semi-infinite metal/dielectric multilayers. Section 3 is

0953-8984/93/407361+14$07.50 © 1993 IOP Publishing Ltd

devoted to the experimental part of this work: preparation and optical characterization of the multilayers by spectrophotometry and infrared spectroscopic ellipsometry. In sections 4 and 5 we present and discuss the experimental optical measurements.

2. Theoretical framework

2.1. Electromagnetic modes in metallic and dielectric monolayers

Radiative surface plasmons can be excited by light at the boundary of a metal whose conduction electrons behave like a gas of nearly free electrons if the electric field vector has a component perpendicular to the boundary, i.e. only for linearly polarized light parallel to the plane of incidence falling on the boundary under non-normal incidence. These surface plasmons are guided waves travelling along the boundary [3]. Non-radiative surface plasmons can also be excited by light using other configurations, but this is not our present interest.

In a metallic thin film these charge oscillations at each interface may interact and produce new radiative and non-radiative plasma modes of multiple orders. The radiative ones, in order to satisfy the energy conservation, must be more or less damped in time and become virtual modes described by complex frequency values whose imaginary part is proportional to the inverse of the lifetime of the virtual mode [4,5]. The fundamental radiative virtual mode is the only one that presents a small radiation damping and can thus be excited and observed experimentally using p polarized light under oblique incidence. For film thicknesses small compared to the wavelength, its frequency is very close to the plasma frequency ω_p of the metal and weakly dependent on the incident light wave vector (i.e. on the angle of incidence).

This mode, already predicted by Ferrell [6] was observed for the first time in Ag layers by Yamaguchi [7], who did not identify it, and then by McAlister and Stern [8], who intepreted it correctly. The dispersion relation of all surface modes in Drude metal films was then extensively studied, for complex frequencies, by Kliewer and Fuchs [9].

The fundamental radiative virtual mode is characterized by a maximum of absorption and reflectance and a minimum of transmittance around ω_p where the real part ε_{rm} of the dielectric function of the metal vanishes while its imaginary part ε_{im} governs the damping due to internal absorption.

By solving the dispersion relation of surface modes in a dielectric or ionic crystal film [10–12], radiative modes were obtained because of polarization effects and lattice vibrations perpendicular to the film occurring around ω_l, the frequency of bulk longitudinal optical mode where ε_{rd} vanishes. These radiative phonon surface polaritons are also virtual modes and can only be excited by p-polarized light under oblique incidence, like radiative surface plasmons.

One obtains, in addition to these modes around ω_l, a series of radiative virtual modes around ω_t, the frequency of the bulk transverse optical mode of the dielectric where ε_{id} undergoes a maximum while ε_{rd} vanishes. These modes correspond to lattice vibrations parallel to the surface of the film and can thus be only excited by light having a component of the electric field parallel to the film, i.e. by s- or p-polarized light under non-normal incidence and also under normal incidence. Notice however that the dispersion relations and consequently these modes are different for p and s polarizations.

Berreman [13] observed experimentally and analysed for the first time these modes in LiF films. He obtained only one of these virtual radiative phonon surface modes around ω_l and another one around ω_t, the others being too much damped by radiation to be observed.

Both modes are characterized by a maximum of absorption and reflectance and a minimum of transmittance. If the dielectric film is deposited on a metal, a minimum of reflectance is then observed at both frequencies. However, the resonance at ω_t is strongly reduced due to the vanishing of the tangential component of the electric field in the metal [14].

2.2. *Effective medium approximation for multilayers*

The dispersion relation of surface radiative modes in metal/dielectric multilayers composed of a finite number of layers of finite thickness has never been solved to our knowledge [15]. Nevertheless, in order to simplify the prediction and the interpretation of the optical properties of such actual media, we have developed the equivalence of these multilayers to a single anisotropic layer with its principal axis normal to the film [16, 17]. The tensor of the equivalent dielectric function thus calculated simplifies greatly in the case of a periodic semi-infinite multilayer composed of films with thickness small compared to the wavelength (EMA):

$$\varepsilon_x = f\varepsilon_m + (1-f)\varepsilon_d$$

$$\varepsilon_z^{-1} = f\varepsilon_m^{-1} + (1-f)\varepsilon_d^{-1}$$

$$f = d_m/(d_m + d_d)$$

where ε_x and ε_z are the components of ε parallel and perpendicular to the plane of the layers, respectively, f is the thickness fraction of the metallic layers in the multilayer, and ε_m, d_m, ε_d and d_d are the dielectric functions and thicknesses of the metallic and dielectric layers respectively.

ε_x presents a metallic character with a vanishing real part at a characteristic frequency $\omega_\parallel$ (analogous to the plasma frequency in metals). When the dielectric function of the metal is given by a Drude model

$$\varepsilon_m(\omega) = P - \omega_p^2/\omega(\omega + i/\tau)$$

the true plasma frequency is thus observed at $\omega_p' = \omega_p/\sqrt{P}$; the expression for $\omega_\parallel$ is

$$\omega_\parallel = \omega_p/\sqrt{P + [(1-f)/f]\varepsilon_d}.$$

$\omega_\parallel$ is always lower than ω_p' of the bulk metal. It increases from 0 eV for $f = 0$ to ω_p' for $f = 1$.

ε_z presents a dielectric character with a vanishing real part at ω_p (analogous to the longitudinal optical frequency in ionic crystals) and a maximum imaginary part at a lower frequency (analogous to the transverse optical frequency in ionic crystals).

The dispersion relation of surface modes has been calculated within the EMA [18, 19] and also for semi-infinite multilayers with layers of finite thickness without retardation [20] and with retardation [19]. Due to the coupling of surface plasmon modes at the metal/dielectric interfaces a window with low reflectance between $\omega_\parallel$ and ω_p in the radiative domain [18, 19] and two sub-bands of quasi-bulk modes in the non-radiative one [20] are predicted. These are the properties in the radiative domain that we discuss further.

3. Experiment

With this aim, we have deposited Ag and SiO_2 monolayers and Ag/SiO_2 periodic multilayers composed of nine layers on glass substrates with different metal fractions f.

The technique of deposition was magnetron sputtering under a base pressure of 2×10^{-7} mbar and an argon residual pressure of 5.9 mbar. The diameter of the Ag and SiO_2 targets was 75 mm. The deposition power was around 80 W and the plasma temperature was lower than 150 °C. The film thicknesses were deduced from the measurements of a quartz oscillator placed in front of the targets in the deposition chamber.

We have performed reflectance (R) and transmittance (T) measurements with polarized light parallel (p) and perpendicular (s) to the plane of incidence under various angles of incidence from 0° to 70° versus frequency from 0.5 eV to 6 eV using a Varian Cary 5 spectrophotometer equipped with a special attachment for reflectance measurements under non-normal incidence.

Ellipsometric measurements under 70° incidence were performed in the infrared (from 0.03 eV to 0.5 eV) by using an original set-up with rotating polarizers coupled to a commercially available Perkin–Elmer Fourier transform spectrometer. A full description of the system can be found elsewhere [21]. The multiplex facility of the Fourier transform spectroscopy is utilized to overcome the low-intensity problem in the infrared.

In brief, we measure the intensities of the following quantities:

(i) from 0.5 eV to 6 eV, R_p and R_s, T_p and T_s, Fresnel reflection and transmission coefficients, relative to the intensity of the polarized light parallel and perpendicular respectively to the plane of incidence; and

(ii) from 0.03 eV to 0.5 eV, $\tan\Psi = (R_p/R_s)^{1/2}$ and $\cos\Delta = \cos(\Delta_p - \Delta_s)$, where Δ_p and Δ_s are the phases of the Fresnel reflection amplitudes.

We have deduced the dielectric function of Ag and SiO_2 used in our multilayers from ellipsometric and photometric measurements performed on single layers prepared in the same conditions as the multilayers. The values are in good agreement with the results in the literature. In particular, the principal characteristic frequencies of these materials, as presented in sections 1 and 2, are indeed observed at $\omega_p = 3.78$ eV for Ag; $\omega_t = 0.133$ eV and $\omega_l = 0.154$ eV for SiO_2.

We present and discuss now the results of some of these optical measurements on the following three multilayers: 9M1515, 9M1522 and 9M1545 composed of nine layers: SiO_2/Ag/SiO_2/Ag/SiO_2/Ag/SiO_2/Ag/SiO_2 on glass substrates with an Ag layer thickness of 15 nm and an SiO_2 layer thickness of 15 nm, 22 nm and 45 nm respectively, corresponding to f values of 0.5, 0.4 and 0.25 respectively.

4. Transparency window and effective medium models

Let us first compare the experimental optical response for p polarized light of a single film of Ag (thickness 50 nm) deposited on SiO_2 (figure 1) with those of our three Ag/SiO_2 multilayers (9M1515 in figure 2, 9M1522 in figure 3 and 9M1545 in figure 4). We focus our discussion on energies below the plasma frequency of Ag, 3.78 eV.

One region with high reflectivity is observed in the single film below the plasma frequency of Ag. This behaviour is not far from the behaviour of bulk Ag, due to the relatively large thickness of the film. In the multilayers, an additional region with lower reflectivity appears between $\omega_{\|}$ (defined in section 2.2) and ω_p. This low-reflectivity region

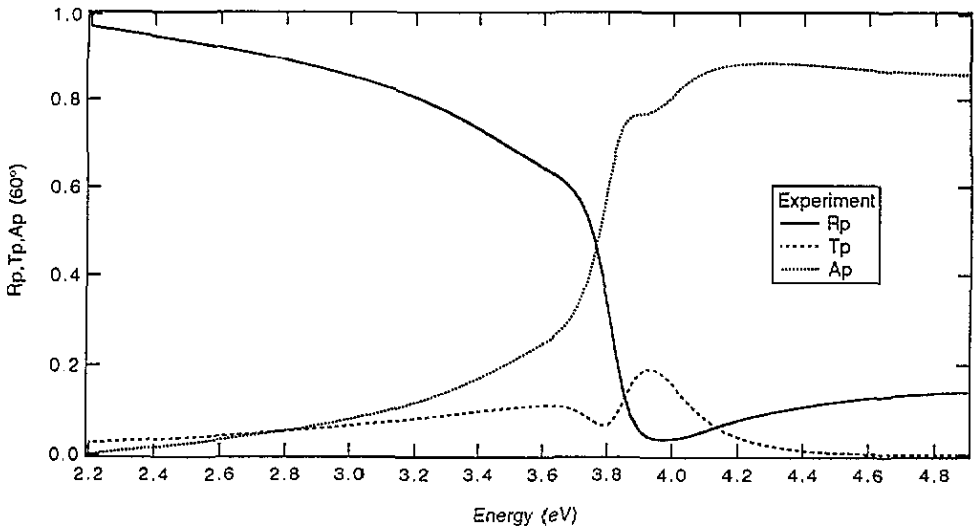

Figure 1. Experimental visible and near-infrared reflectance, transmittance and absorption for p polarized light, under 60° incidence, of a single Ag film (thickness 50 nm) deposited on a glass substrate.

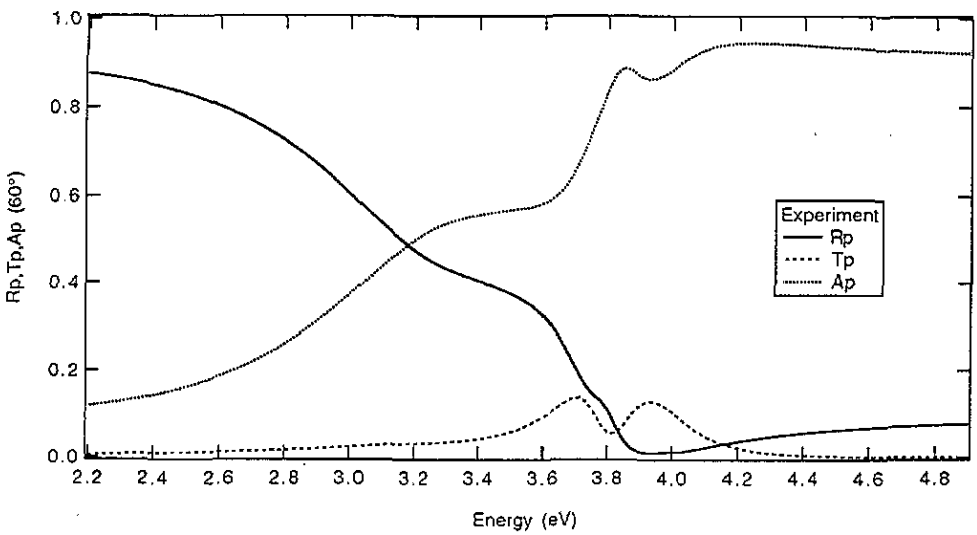

Figure 2. Experimental visible and near-infrared reflectance, transmittance and absorption for p polarized light, under 60° incidence, of an Ag/SiO_2 multilayer composed of four Ag layers of 15 nm alternated with five SiO_2 layers of 15 nm (9M1515, $f = 0.5$) deposited on a glass substrate.

corresponds to a transparency window (clearly visible on the experimental transmittance curves) associated with a propagative mode in the multilayer (the imaginary part of the Bloch wave vector is close to zero in this region). This propagative mode results from the coupling of surface plasmon modes at the metal/dielectric interfaces.

The frequency $\omega_{\parallel}$ of the reflectivity edge follows the metal fraction in the multilayers

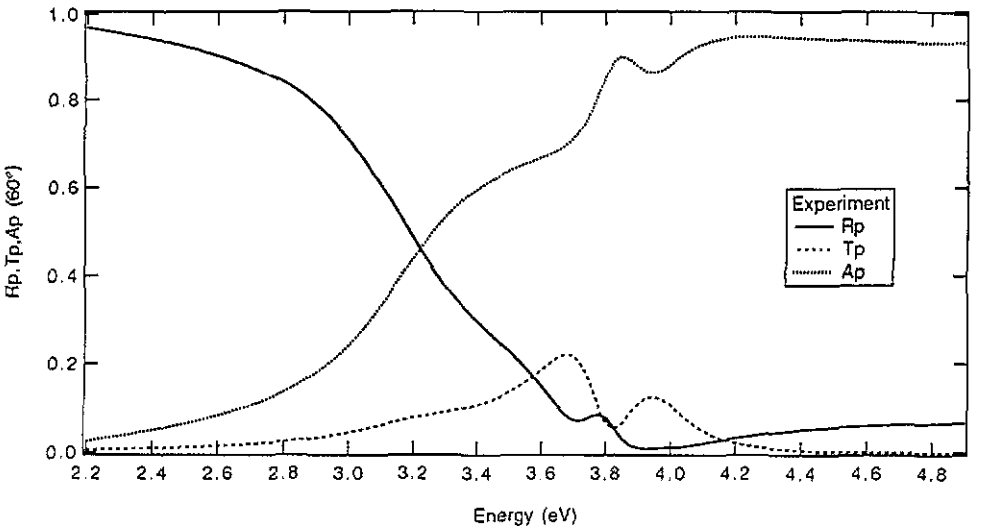

Figure 3. Experimental visible and near-infrared reflectance, transmittance and absorption for p polarized light, under 60° incidence, of an Ag/SiO_2 multilayer composed of four Ag layers of 15 nm alternated with five SiO_2 layers of 22 nm (9M1522, $f = 0.4$) deposited on a glass substrate.

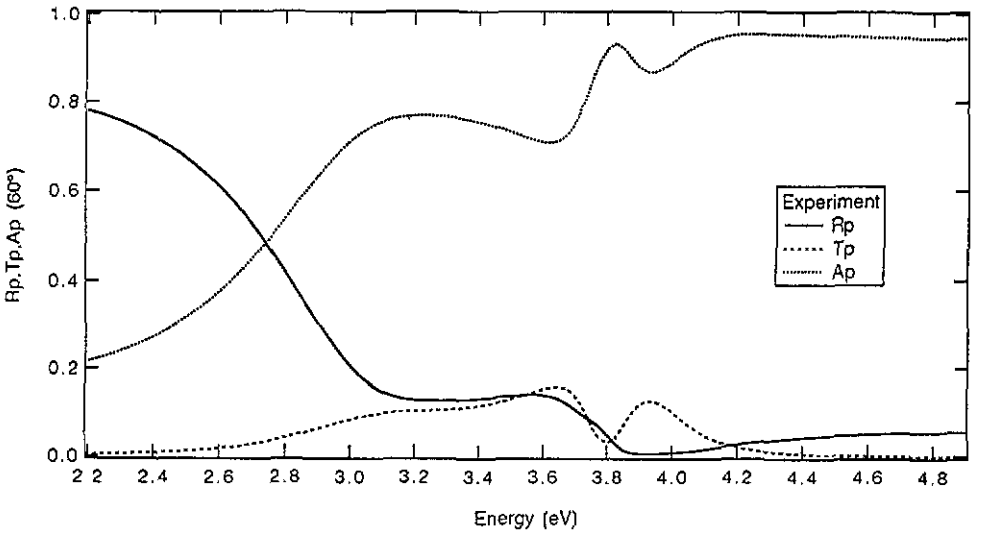

Figure 4. Experimental visible and near-infrared reflectance, transmittance and absorption for p polarized light, under 60° incidence, of an Ag/SiO_2 multilayer composed of four Ag layers of 15 nm alternated with five SiO_2 layers of 45 nm (9M1545, $f = 0.25$) deposited on a glass substrate.

($f = 0.5$ in 9M1515, $f = 0.4$ in 9M1522, $f = 0.25$ in 9M1545) according to EMA predictions (see section 2.2 and table 1). It corresponds to the vanishing of the real part of the xx component (parallel to the films) of the dielectric function tensor calculated within this approximation. Although our multilayers were composed of a small number (nine) of

layers of optical thickness not very small compared to the wavelength, our experimental results concerning $\omega_{\parallel}$ are in good agreement with this EMA calculation valid for semi-infinite media (see figure 5). It can indeed be demonstrated using a full multilayer calculation that the transparency window appears even for seven layers (with our experimental thicknesses), with its edges at $\omega_{\parallel}$ and ω_p values predicted by the EMA.

Table 1. Values of $\omega_{\parallel}$ calculated within the EMA and measured from our experimental results as the position of the decreasing reflectivity edge for the different metal fractions in our multilayers.

f	$\omega_{\parallel}$ (EMA)(eV)	$\omega_{\parallel}$ (experimental)(eV)
0.25	2.696	2.642
0.4	3.104	3.100
0.5	3.428	3.287

5. Electromagnetic radiative modes and coupling

5.1. Visible range

Let us now focus the discussion on the three extrema of the optical properties observed around the plasma frequency of Ag, $\omega_p = 3.78$ eV, in both the single Ag film and the three multilayers.

The four transmittance curves in figures 1, 2, 3 and 4 exhibit a minimum at ω_p. This corresponds to the excitation of the fundamental radiative virtual mode in a single Ag layer. This radiative surface plasmon, described in section 2, presents an antisymmetric configuration of charges at the two interfaces of the Ag layer. These experimental results (and others not presented here) show that the frequency of this mode is almost independent of the angle of incidence and of the thickness of the dielectric (see figure 6) and metallic films. However, the intensity of the optical response depends strongly on these parameters (see figure 7 for the angular dependence).

This mode is also characterized by a maximum of reflectance and absorption. Due to the relatively high value of the imaginary part of the dielectric function of the metal ($\varepsilon_{im} = 0.358$), the maximum of reflectance is very weak (for the Ag layer thickness of 15 nm used throughout this study). Replacing the dielectric function of Ag by a Drude formula (neglecting the interband contribution) gives a much lower value of ε_{im} ($\varepsilon_{im} = 0.185$) at 3.78 eV. A simulation using this Drude value produces a strong enhancement of this maximum of R_p (see figure 8). Experimentally this can only be observed in our results on the 9M1522 multilayer (figure 3). It can be explained by optimal coupling conditions and also by interfacial effects due to the deposition process.

Another important effect of the interband transitions in Ag is the occurrence of a maximum of transmittance associated with a minimum of reflectance and absorption around 3.87 eV clearly visible in the single Ag film and in the multilayers (figures 1, 2, 3 and 4). These extrema are absent in the simulation using a Drude formula for the metal (figure 8). They can be interpreted as the manifestation of an electromagnetic mode with Brewster character. A more detailed analysis of this mode is presented elsewhere [22] in the case of a single Ag film, by solving the dispersion relation for complex values of the frequency. It notably demonstrates the symmetric character of this mode and the dependence of its frequency on the angle of incidence. In the multilayer its frequency is moreover independent

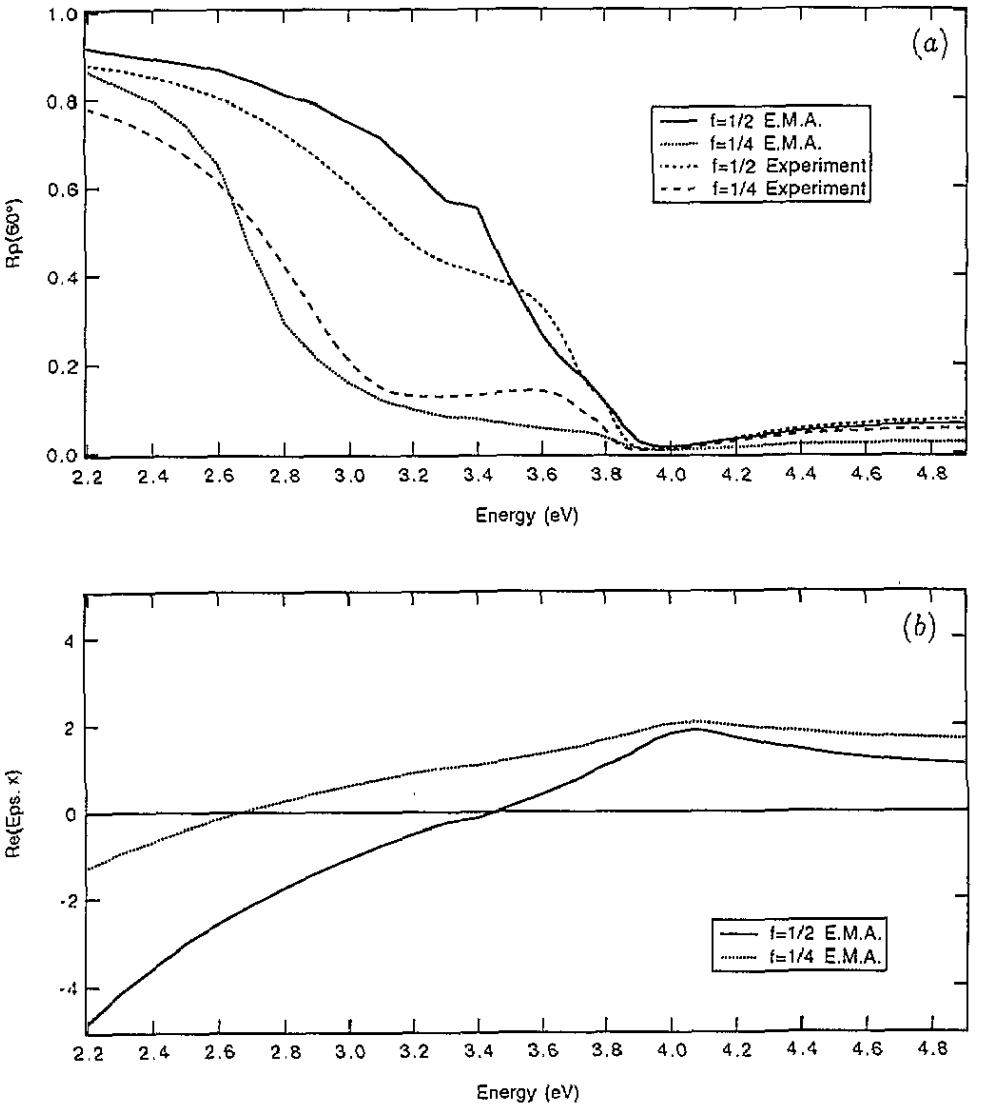

Figure 5. Experimental visible and near-infrared reflectivity for p polarized light, under 60° incidence, of the 9M1515 ($f = 0.5$) and 9M1545 ($f = 0.25$) Ag/SiO_2 multilayers on glass substrates compared to their reflectivity: (*a*) calculated within the EMA using our experimental data for Ag and SiO_2; (*b*) real part of the component (parallel to the films) of the dielectric function tensor calculated within the EMA approximation.

of the thickness of the metallic and dielectric films. The maximum of T_p at this frequency depends on all these parameters, it is but very weakly dependent on the thickness of the dielectric films (see figure 6).

Below ω_p another maximum of transmittance is observed around 3.65 eV. It depends on the same parameters as the extrema around 3.87 eV, but it differs by a strong dependence of its intensity on the thickness of the dielectric layers (see figure 6). This confirms the coupling between metallic layers through the dielectric ones in the multilayers. We have presently no clear interpretation of this extremum. It does not seem to satisfy the dispersion

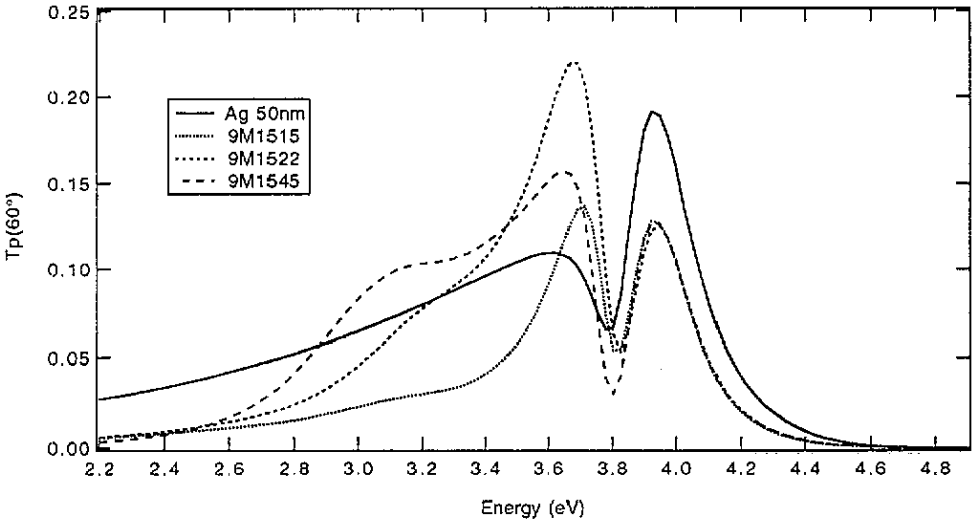

Figure 6. Experimental visible and near-infrared transmittance for p polarized light, under 60° incidence, of a single Ag film (thickness 50 nm) and the three Ag/SiO_2 multilayers: 9M1515 ($f = 0.5$), 9M1522 ($f = 0.4$), 9M1545 ($f = 0.25$) deposited on glass substrates.

relation of Brewster modes like the extremum around 3.87 eV.

In order to clarify these coupling effects between metallic films through the dielectric ones at the three characteristic frequencies pointed out above (around 3.65 eV, at 3.78 eV and around 3.87 eV), we have simulated the transmittance (p polarization, incidence 60°) of a multilayer analogous to our experimental ones (figure 9) at these frequencies versus the thickness of the SiO_2 layers (of real constant dielectric function equal to 2.25) by using for the dielectric function of the metallic layers the value determined on the single Ag layer presented in this paper and also by using a Drude model, at 3.87 eV.

The minimum of $T_p(60°)$ occurring at $\omega_p = 3.78$ eV is very weakly dependent on the thickness of the dielectric layers. Its amplitude of variation is less than 5%.

The maximum around 3.87 eV, which is induced by interband transitions in actual Ag (Brewster mode), is also weakly dependent on the dielectric thickness (amplitude less than 3%), whereas the value of the transmittance calculated with the Drude model (which does not exhibit any maximum versus frequency) shows variations larger than 14%.

Around 3.65 eV the maximum of $T_p(60°)$ exhibits strong oscillations versus the dielectric thickness. This coupling effect is simply an interference effect in the dielectric layers (short oscillations) and in the whole multilayer (long oscillations).

These predicted behaviours are in good agreement with our experimental measurements under oblique incidence for p polarization (figure 6). It is also worth noting that, as expected, none of the optical measurements (R, T, A) for s polarization exhibits any peculiar behaviour at the characteristic frequencies pointed out above.

5.2. Infrared range

The optical properties of our multilayers were studied in the visible and the infrared by spectroscopic ellipsometry [23]. We discuss below the infrared results.

A strong feature shows up in the ellipsometric parameters close to the longitudinal optical frequency of SiO_2 determined above, i.e. at $\omega_l = 0.154$ eV.

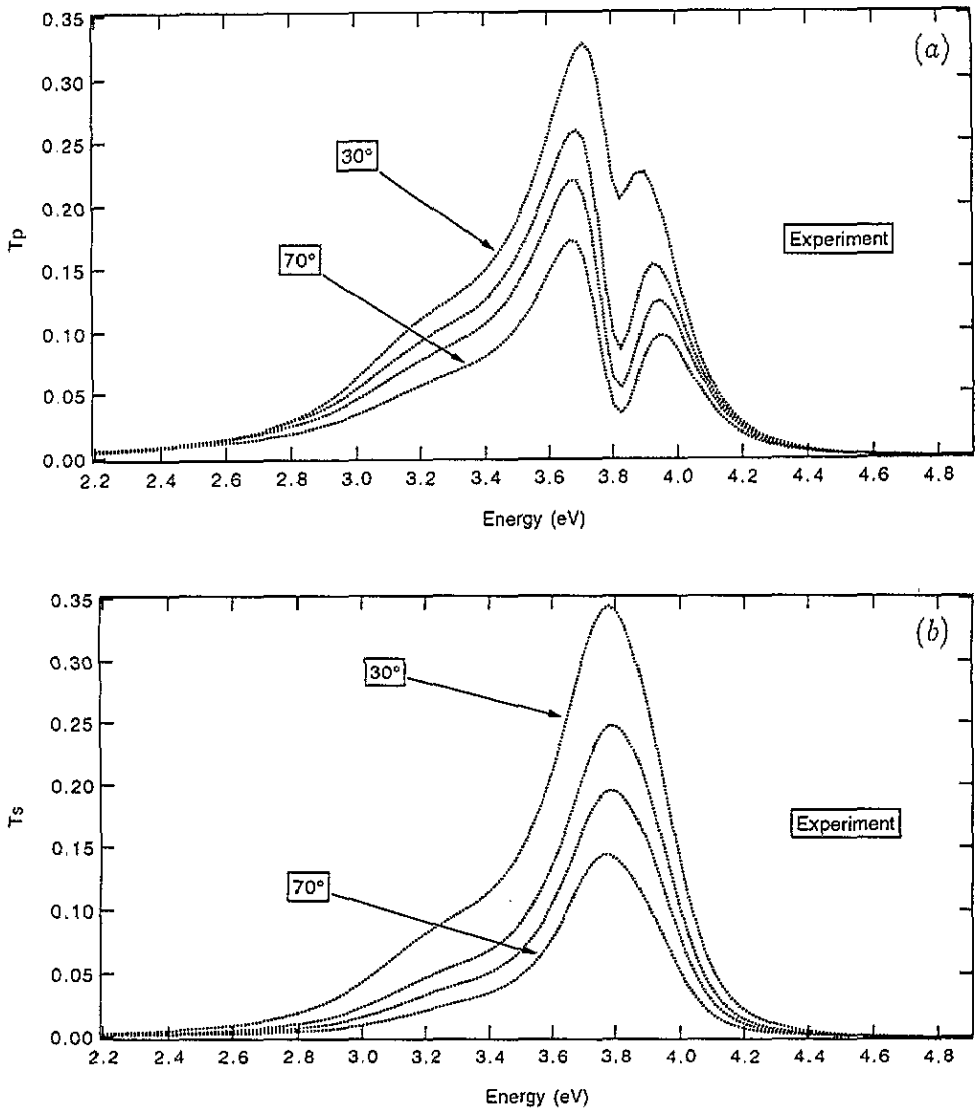

Figure 7. Experimental visible and near-infrared transmittance under variable angle of incidence (30°, 50°, 60° and 70°) for p polarized light (*a*) and s polarized light (*b*) of an Ag/SiO_2 multilayer composed of four Ag layers of 15 nm alternated with five SiO_2 layers of 22 nm (9M1522, $f = 0.4$) deposited on a glass substrate.

In figure 10(*a*), $\tan\Psi$ shows a minimum, the depth of which decreases with the SiO_2 thickness which governs the strength of the Berreman resonance, as already noted in section 2. It is indeed the 9M1545 multilayer, which has the largest dielectric thickness, that exhibits the deepest resonance. Cos Δ in figure 10(*b*) exhibits a plateau between ω_t and ω_l (0.133 eV and 0.154 eV) with a steep edge at ω_l. The level of the plateau depends on the dielectric layer thickness, like the minimum in $\tan\Psi$. Both features are more pronounced in the 9M1545 multilayer, where the dielectric layer thickness is closer to the Berreman thickness, evaluated to 300 nm by using Berreman's formula [14] for a single SiO_2 layer on Ag with an imaginary part of the dielectric function of SiO_2 equal to 0.6 at ω_l (our

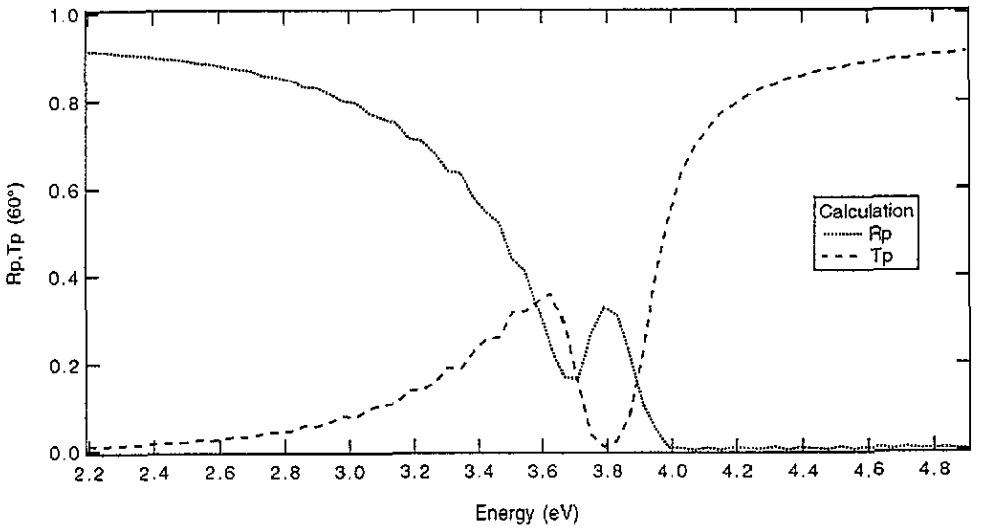

Figure 8. Calculated visible and near-infrared reflectance and transmittance for p polarized light, under 60° incidence, of an Ag/SiO_2 multilayer composed of four Ag layers of 15 nm alternated with five SiO_2 layers of 15 nm (9M1515, $f = 0.5$) deposited on a glass substrate. Dielectric function of Ag; Drude ($P = 7$, $\omega_p = 10$ eV, $\omega_\tau = 0.1$ eV); dielectric function of SiO_2; 2.25.

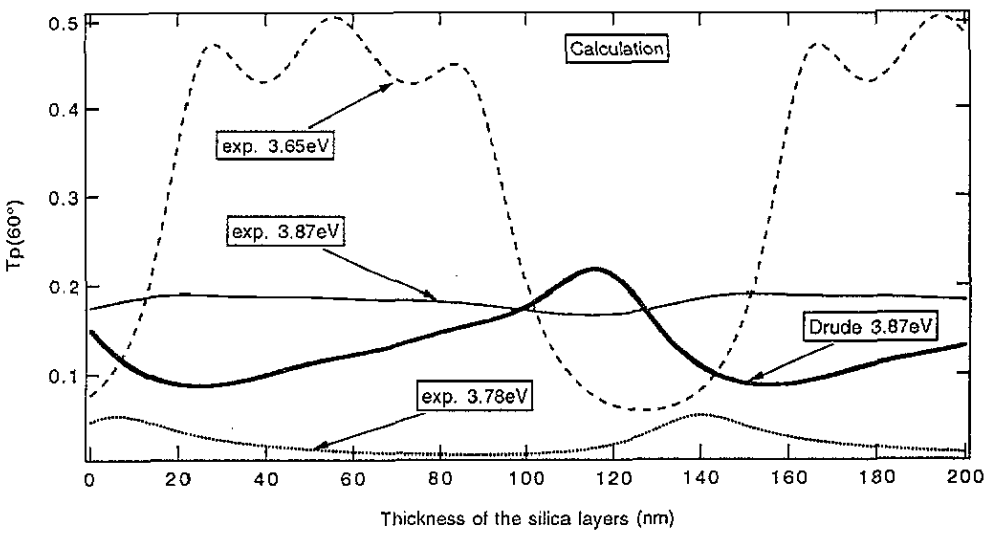

Figure 9. Calculated transmittance for p polarized light, under 60° incidence, versus the thickness of the silica layers, at the frequencies 3.65 eV, 3.78 eV and 3.87 eV of an Ag/SiO_2 multilayer composed of four Ag layers (15 nm) alternated with five SiO_2 layers (variable thickness) deposited on a glass substrate. The data for Ag correspond to our experimental values, except for the bold full curve where a Drude model ($P = 7$, $\omega_p = 10$ eV, $\omega_\tau = 0.1$ eV) has been used.

experimental value).

In order to establish whether this effect results from an enhancement due to the multilayer structure, we have performed simulations of $\tan\Psi$ (at 70° incidence) at the frequency ω_1

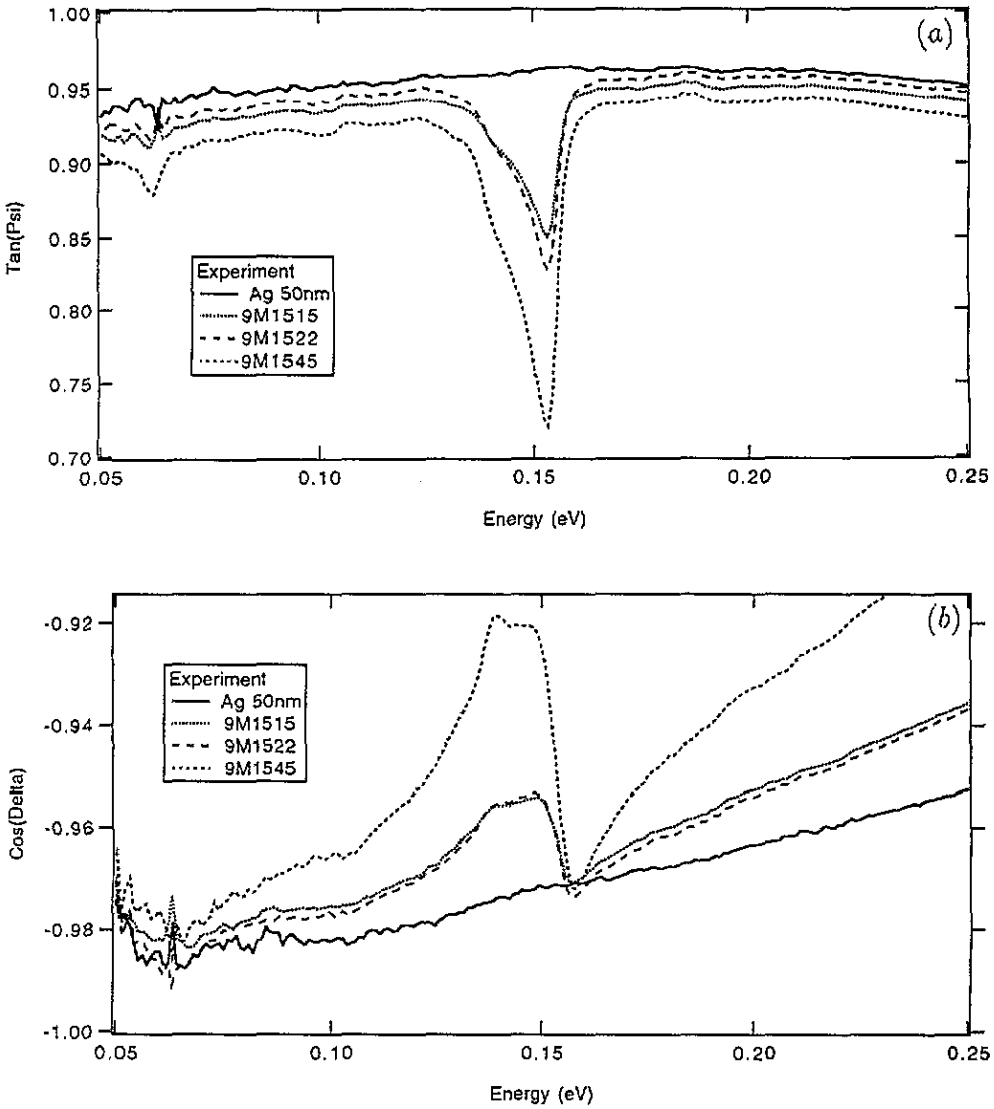

Figure 10. Experimental infrared ellipsometric parameters $\tan\Psi$ (*a*) and $\cos\Delta$ (*b*), under 70° incidence, of an Ag monolayer of 50 nm and of three Ag/SiO_2 multilayers composed of four Ag layers of 15 nm alternated with five SiO_2 layers of 15 nm (9M1515), 22 nm (9M1522) and 45 nm (9M1545) deposited on glass substrates.

for a multilayer and for one double layer (SiO_2 on Ag) with variable SiO_2 thickness and an Ag thickness equal to 15 nm (see figure 11). The two curves are exactly the same and exhibit a flat minimum around 240 nm. This thickness is little smaller than the calculated Berreman thickness (300 nm) due to some inaccuracy in the determination of the infrared dielectric function of SiO_2, which is the main parameter of the calculation. The identity between the two curves suggests that the effect observed in the multilayer is almost entirely due to the first two layers (SiO_2 and Ag) due to the very high infrared reflectance of the first Ag layer. There is thus no coupling of the Berreman mode in the multilayer. One can also notice that the calculated values of $\tan\Psi$ at ω_l (figure 11) are in good agreement with

our measurements (figure 10(*a*)). According to Berreman's predictions in single dielectric layers (see section 2.1) the mode at ω_t is observed but only weakly due to the presence of the metallic sublayer.

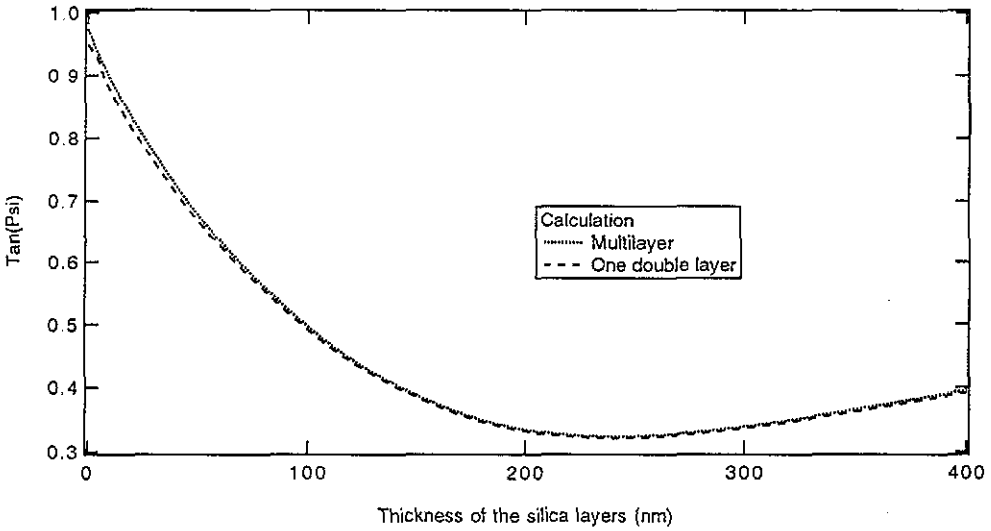

Figure 11. Calculated infrared ellipsometric parameter tan Ψ, under 70° incidence, versus the thickness of the SiO_2 layers, at the longitudinal frequency of SiO_2 of an Ag/SiO_2 multilayer composed of four Ag layers (15 nm) alternated with five SiO_2 layers (variable thickness) on a glass substrate and of one Ag/SiO_2 double layer (Ag, 15 nm; SiO_2, variable thickness) on a glass substrate.

6. Conclusion

The following points result from this discussion of the optical properties of actual Ag/SiO_2 multilayers composed of nine layers with different thicknesses of SiO_2.

(i) All radiative virtual modes already predicted and observed in single metallic or dielectric layers have been characterized in our multilayers. Near the Ag plasma frequency the fundamental mode (less damped by radiation) is weakly affected by the multilayer structure, like the Brewster mode observed around 3.87 eV. In the infrared around the longitudinal and transverse optical frequencies of SiO_2 the Berreman modes we observe are exactly those predicted in an SiO_2/Ag bilayer due to the high reflectivity of the thin Ag layers at these frequencies. On the other hand the maximum of transmittance observed around 3.65 eV can be strongly enhanced by varying the SiO_2 thickness in the multilayer. Although this extremum of the optical properties presented all the characteristics of a Brewster mode, it is not given by the dispersion relation of these modes in a single Ag layer and must be attributed to interference effects.

(ii) The coupling effect of the surface plasmon modes throughout the multilayer has been clearly demonstrated by observing in the visible range the transparency window occurring in the radiative domain, the width of which follows the predictions of the EMA.

(iii) Most of the phenomena described above are only observed for p polarization and thus induce strong anisotropic effects. These metal/dielectric multilayers can thus

advantageously replace natural anisotropic crystals for specific applications. Moreover, the flexibility of some of their optical properties versus the dielectric thickness (extrema around 3.65 eV and width of the transparency window), make these materials suitable for applications to selective coatings.

Acknowledgments

We would like to thank Dr R Krishnan and Mr M Tessier for sample preparation, Professor O Hunderi and Dr E Wold for infrared ellipsometric measurements, Professor P Gadenne and Exxon Co. for the utilization of their reflectance accessory, and Professors O Hunderi, R G Barrera and P Sheng for fruitful discussions.

References

[1] Youn K B, Sella C, Barchewitz R, Arbaoui M and Alehyane N 1990 *Opt. Commun.* **77** 256
[2] Chauvineau J P, Como J, Naccache D, Nevot L, Pardo B and Valiergue L 1984 *J. Opt.* **15** 265
[3] Raether H 1977 *Physics of Thin Films* vol 9 (New York: Academic)
[4] Economou E N and Ngai K L 1974 *Aspects of the Study of Surfaces, Advances in Chemical Physics* vol 27, ed I Prigogine and S Rice (New York: Wiley) p 265
[5] Kliewer K L and Fuchs R 1974 *Aspects of the Study of Surfaces, Advances in Chemical Physics* vol 27, ed I Prigogine and S Rice (New York: Wiley) p 355
[6] Ferrell R A 1958 *Phys. Rev.* **111** 1214
[7] Yamaguchi S 1962 *J. Phys. Soc. Japan* **17** 1172
[8] McAlister A J and Stern E A 1963 *Phys. Rev.* **132** 1599
[9] Kliewer K L and Fuchs R 1967 *Phys. Rev.* **153** 498
[10] Kliewer K L and Fuchs R 1966 *Phys. Rev.* **144** 495
[11] Kliewer K L and Fuchs R 1966 *Phys. Rev.* **150** 573
[12] Kliewer K L and Fuchs R 1966 *Phys. Rev.* **150** 589
[13] Berreman D W 1963 *Phys. Rev.* **130** 2193
[14] Harbecke B, Heinz B and Grosse P 1985 *Appl. Phys.* A **38** 263
[15] Welch H, Lafait J and Bichri A to be published
[16] Lafait J, Yamaguchi T, Figerio J M, Bichri A and Driss-Khodja K 1990 *Appl. Opt.* **29** 2460
[17] Yamaguchi T, Lafait J, Bichri A and Driss-Khodja K 1991 *Appl. Opt.* **30** 489
[18] Hunderi O 1987 *J. Wave-Mater. Interact.* **2** 29
[19] Mochan W L, del Castillo-Mussot M and Barrera R G 1987 *Phys. Rev.* B **35** 1088
[20] Camley R E and Mills D L 1984 *Phys. Rev.* B **29** 1695
[21] Bremer J, Hunderi O, Fanping K, Skauli T and Wold E 1992 *Appl. Opt.* **31** 471
[22] Gadenne P, Gadenne M, Lafait J, Sheng P, Zhou M and Ruppert F to be published
[23] Bichri A, Hunderi O, Lafait J and Wold E 1993 *Thin Solid Films* at press